# Radiocarbon analyses along the EDML ice core in Antarctica

*By* R. S. W. VAN DE WAL[1]*, H. A. J. MEIJER[2], M. DE ROOIJ[2] and C. VAN DER VEEN[1],
[1]*Institute for Marine and Atmospheric research Utrecht, Utrecht University, PO box 80005, 3508 TA Utrecht, The Netherlands;* [2]*Center for Isotope Research, University of Groningen, Nijenborgh 4 9747 AG Groningen, The Netherlands*

ABSTRACT

Samples, 17 in total, from the EDML core drilled at Kohnen station Antarctica are analysed for $^{14}CO$ and $^{14}CO_2$ with a dry-extraction technique in combination with accelerator mass spectrometry. Results of the in situ produced $^{14}CO$ fraction show a very low concentration of in situ produced $^{14}CO$. Despite these low levels in carbon monoxide, a significant in situ production is observed in the carbon dioxide fraction. For the first time we found background values for the ice samples which are equal to line blanks. The data set is used to test a model for the production of $^{14}C$ in the ice matrix, in combination with a degassing as $^{14}CO_2$ and possibly as $^{14}CO$ into the air bubbles. Application of the model, for which no independent validation is yet possible, offers the opportunity to use radiocarbon analysis as dating technique for the air bubbles in the ice. Assigning an arbitrary error of 25% to the calculation of the in situ production leads to age estimates, after correction for the in situ production, which are in agreement with age estimates based on a volcanic layer match of EDML to the Dome C timescale in combination with a correction for firn diffusion.

## 1. Introduction

The radionuclide $^{14}C$ can be incorporated in ice in two ways, firstly by trapping of atmospheric gases during the accumulation and secondly through in situ production by cosmic rays. Trapped atmospheric $^{14}CO_2$ offers the possibility of dating, but fast neutrons and muons produce contaminating $^{14}C$ in nuclear reactions on oxygen in snow and ice. This additional $^{14}C$ is oxidized to $^{14}CO$ and $^{14}CO_2$. This process offers the possibility to determine the ablation rate in blue ice areas in Antarctica, but complicates radiocarbon dating of ice cores, which is the ultimate goal of the $^{14}C$ analyses along ice cores from an accumulation zone, like the one presented in this paper.

The presence in ice of in situ produced $^{14}C$ has been confirmed in several experiments (Lal and Jull, 1990; Jull et al., 1994; Van de Wal et al., 1994) indicating production by neutrons. Presence of additional $^{14}C$ below 10 meters in blue ice can be ascribed to muon capture in $^{16}O$ (Van der Kemp et al., 2002). Based on this work it was believed that radiocarbon dating of ice was feasible because there were indications for a constant ratio between in

situ produced $^{14}CO$ and $^{14}CO_2$, which offers the possibility to correct for in situ produced $^{14}CO_2$. The prospects of radiocarbon dating increased by results from firn cores by Smith et al. (2000) and Van der Kemp et al. (2000) both indicating very low $^{14}CO$ concentrations in the accumulation zone of an ice sheet. If there is indeed a constant ratio between $^{14}CO$ and $^{14}CO_2$ in situ, a low $^{14}CO$ activity would imply a barely enhanced $^{14}CO_2$ level and hence the possibility of dating. Results for deeper ice samples from Dome C (De Jong et al., 2004) did not conclusively confirm this as many of the samples failed to produce good results and some of the remaining samples showed activity from postcoring in situ production, due to exposure to cosmic rays at the surface near Dome C. So based on previous cores from the accumulation zone it was believed that radiocarbon dating was feasible, provided that postcoring in situ production could be prevented.

Against this background we analysed 17 samples with a dry extraction technique from the EDML core, which was drilled in Dronning Maud Land (DML) as part of the European Project for Ice Coring in Antarctica (EPICA). It is the first deep ice core from the Eastern Antarctic plateau with many successful radiocarbon samples providing us more insight in $^{14}C$ in ice than ever before. Based on the result we propose a new model to correct the $^{14}C$ measurements for in situ production, which evidently shows up at depth in ice from the accumulation zone despite the low $^{14}CO$ concentrations.

*Corresponding author.
e-mail: wal@phys.uu.nl

## 2. Experimental procedure

Ice samples were taken from the EDML core at Kohnen station (75°00′S, 00°04′E, 2892 m.a.s.l.) in Antarctica. Gases were extracted from the ice samples, weighing approximately 3 kg, using a dry-extraction technique. The apparatus and the experimental procedure have been described in detail elsewhere (Van Roijen et al., 1994, Van Roijen 1996 and Van der Kemp et al., 2000). The $^{14}C$ measurements are performed on both the CO and the $CO_2$ fraction of the extracted air, for which we have a 100% extraction efficiency. Prior to an extraction we added $^{14}C$-free CO carrier gas ( $\approx 220$ $\mu$g C). In the extraction procedure the ice is milled in an evacuated recipient mounted in a freezing box at −30 °C. The released $CO_2$ is collected in a cooling trap with liquid $N_2$, while the other gases are passing to another unit, where the CO is converted into $CO_2$, with oxygen and a hot platinum wire (∼400 °C), and subsequently trapped. Vapour of drilling fluid (D40 + HCFC − 141b) was removed with a cryogenic trap at −130°C, at which temperature $CO_2$ evaporates while the contaminant remains frozen. All $CO_2$ samples are diluted by a factor of 5–7 with a $^{14}C$ free gas to obtain a sample mass of 200 $\mu$g C. On the one hand, dilution increases the uncertainty in the result for the original sample (this uncertainty increases linearly with the dilution factor, see Appendix). On the other hand, however, it increases the reliability and accuracy of the measurements as such. After intensive tests with the CIO-Groningen AMS facility, samples of around 200 $\mu$g C appeared to be the best compromise between still acceptable dilution factors on the one hand, and useful total accuracies and high reliability on the other. Details on the dilution procedure are presented in the Appendix.

The resulting two $CO_2$ fractions were converted into graphite and their $^{14}C/^{12}C$ and $^{13}C/^{12}C$ ratios were simultaneously measured with the AMS facility of the Centre for Isotope research University of Groningen (CIO). From these ratios, corrected for (laboratory) fractionation and contamination effects, the $^{14}C$ activities of the samples were deduced and normalized to $\delta^{13}C = -25 ‰$ w.r.t. VPDB (Mook and Van der Plicht, 1999). Corrections for laboratory contamination have been derived from line blanks representing not only graphitization and AMS measurement, but also the gas extraction procedure (Van Roijen et al., 1994 and Van der Kemp et al., 2000). The CO and $CO_2$ samples are corrected for an average background of $0.08 \pm 0.15$ and $0.33 \pm 0.17$ pmC, respectively. The $^{14}C$ ages are converted into Calendar years using the Groningen calibration program (Van der Plicht, 1993), which uses the Intcal04 data set (Reimer et al., 2004).

## 3. Results

Of the available original 18 ice samples one failed due to a leakage in the extraction system. The remaining 17 available samples gave successful results for $^{14}CO_2$. Fifteen of these also provided a reliable $^{14}CO$ result, which is important for the study of the in
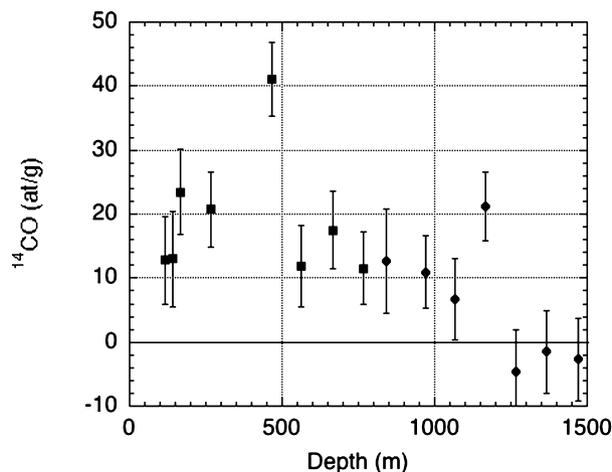


*Fig. 1.* The $^{14}C$ concentration (at g$^{-1}$ ice) of the CO fraction as a function of the depth, indicating an activity above the background, which is not evidently depending on the depth.

situ $^{14}C$ production. Natural CO concentrations in air and hence in ice are so low that all the extracted $^{14}C$ from this fraction (<2 at/g ice) can safely be assumed to originate from in situ production. Figure 1 shows the results for the EDML core. The figure shows that the amount of $^{14}CO$ is slightly above the background level caused by the analyses itself, with an average of $13 \pm 9$ at/g ice (corresponding to 0.4 pmC). This result is in agreement with earlier results by Van der Kemp et al. (2000), who found with the same extraction technique $9 \pm 6$ at/g ice. Smith et al. (2000) found values of $29 \pm 9$ at/g ice with a different dry extraction method. Results where melting techniques are used report usually higher values. Close observation of the figure shows two clear outliers for which we have no explanation. Although the measurements seem to indicate a decay-related decrease over time, correcting the results for the decay does not significantly decrease the scatter. This means that we cannot simply discriminate whether this small though significant amount of $^{14}CO$ has been formed during deposition of snow, in the ice, or after extraction of the ice core.

Results for the $^{14}CO_2$ fraction are shown in Figure 2 and in Table 1. Clearly, the activity decreases with the age of the samples. The span is from above modern (110 pmC) to not significantly different from the background for samples, which are supposed to be older than 35 kyr BP. The $^{14}CO_2$ activities are presented as a function of the air age of the samples. This air age is obtained by correcting with a firn diffusion model for the difference between matrix and air phase to the dating of the EDML core, which is based on a volcanic match of EDML and the Dome C core. The Dome C timescale is known as the EDC3beta4 scale and refers to the matrix. The correction term for the delta age ranged from around 700 years for Holocene samples to 1800 years for Pleistocene samples. The calculated air age was converted to a $^{14}C$ activity in pmC, which is shown for reference in
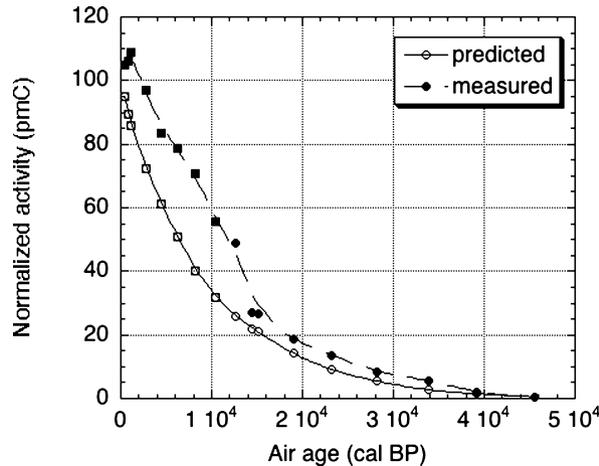
*Fig. 2.* The normalized activity (in pmC) for the $^{14}CO_2$ fraction of the samples as a function of predicted air age (EDC3beta4, see text). As a reference we also show the atmospheric $14CO_2$ corresponding with that age.

Fig. 2 as well, and labeled as 'predicted'. The difference between measured and predicted values reaches a maximum of 30 pmC somewhere between 5000 and 10 000 years BP. This difference cannot be attributed to errors in the measurements (1–2 pmC) or errors in the age-scale (1–2 kyr). Uncertainties in the firn air correction are not important. From Fig. 2 we have to conclude that the air bubbles in the ice contain an additional $^{14}CO_2$ component, which varies with the age of the ice. The question is: what causes this additional $^{14}CO_2$?

In order to study this the amount of extra $^{14}C$ in the $CO_2$ fraction results are compared to the $^{14}C$ from the CO fraction. Earlier work for blue ice areas as well as work done for ice from accumulation zones, but with different extraction techniques, suggested a fixed ratio of in situ $^{14}C$ between the $^{14}CO$ and $^{14}CO_2$ fraction (e.g. Roessler, 1988; Lal and Jull, 1990; Van der Kemp et al., 2002). Combining the results from the $^{14}CO$ and excess $^{14}CO_2$ as presented in the Figs 1 and 2 allows us to calculate this ratio. Figure 3 shows the $^{14}CO_2/^{14}CO$ ratio for the EDML core as a function of the depth. These results show somewhat higher ratios for younger ice and lower ratios for older ice. Despite the considerable errors there seems little evidence for a constant ratio. A constant ratio is in fact excluded at first sight because the difference between predicted and measured activity of the $^{14}CO_2$ varies over time, whereas the $^{14}CO$ activity remains more or less constant (see Table 1). Despite the changing difference between predicted and measured activity we observe a clear though not linear relation between the two as shown in Fig. 4.

## 4. Discussion

The data highlight several points:

(1)  Low $^{14}CO$ concentrations indicate that marked contamination due to postcoring in situ production can be excluded.

(2)  There is no clear evidence for a constant ratio between in situ $^{14}CO_2$ and $^{14}CO$ in the released gases.

(3)  There is an excess of $^{14}CO_2$ relative to the expected level, which shows a clear time dependent signature.

(4)  Predicted activities and measurements show a high, although not linear correlation.

In what follows we propose a model, which can explain these observations. Its basic idea is that there is a huge reservoir of $^{14}C$ in the firn matrix. Based on the equations given by Lal et al. (1987) we calculated a saturation level of $^{14}C$ for this site, which is about eight times the amount of $^{14}C$ included in the air bubbles of modern ice. The crucial question is: what happens with this reservoir? One extreme case is full ventilation before pore close off. This would lead to no additional $^{14}C$ at all in the measurements, which is clearly not the case. The other extreme case is that the in situ produced $^{14}C$ stays forever in the matrix. In that case we would not observe increased levels of $^{14}CO_2$ either. Reality is that we find a small increase (not a factor 8). This leads us to propose the following mechanism: $^{14}C$ atoms are produced in the firn and slowly released with time in the form of $^{14}CO_2$ and possibly $^{14}CO$, which we neglect here for the moment. This leads to an increasing amount of in situ $^{14}CO_2$ over time. As this process starts as soon as the snow is deposited it means that the absolute amount of in situ $^{14}CO_2$ will decrease over time due to decay after saturation has been reached. This means that there are two counteracting mechanisms for the $^{14}CO_2$ activity in the air bubbles: the release from the matrix leading to an increase and the $^{14}C$ decay leading to a decrease. Depending on the rate factors there will be a maximum in the $^{14}CO_2$ concentration in the air at some time. The latter is qualitatively in agreement with the measurements presented in this paper indicating a maximum difference between 5 and 10 kyr BP (see Fig. 2).

Based on the processes described above we formulate the following model for the $^{14}CO_2$ concentration in ice. The total amount I of in situ produced $^{14}CO_2$ is split into two fractions.

$$I = I_m + I_a. \tag{1}$$

The subscripts m and a indicate the amount enclosed in the matrix and in the air bubbles, respectively. The change of the amount in the matrix is caused by two processes radioactive decay and degassing to the air:

$$\frac{dI_m}{dt} = -\lambda I_m - \gamma I_m, \tag{2}$$

where $\lambda$ is the decay constant of $^{14}C$ and $\gamma$ is the $CO_2$ degassing rate. The assumption is that degassing depends on the amount of $^{14}C$ included. This equation implies that the change in the amount in the air is given by:

$$\frac{dI_a}{dt} = +\gamma I_m - \lambda I_a. \tag{3}$$

Integration of eqs (2) and (3) leads to:

$$I_m(t) = I_{m,0} e^{-(\lambda+\gamma)t} \tag{4}$$

*Table 1.*    Results of the $CO_2$ fraction of the samples. Cal BP = 1950-cal AD, being calendar years before 1950. xx not to be determined. Sample 782-783 suffered from a leakage in the extraction system. Calibration data of Reimer et al. (2004) are used to obtain the calibrated ages. In case the calibration resulted in an interrupted $1\sigma$ range, the part containing the peak value for the calibrated age is given first.

| GrA nr | Depth in EDML core (m) | Activity CO (pmC) | Activity $CO_2$ (pmC) | $^{14}C$ age (yrs BP) | Calibrated $1\sigma$ − range (AD/BC) |
|---|---|---|---|---|---|
| 28 528 | 118–119 | $0.3 \pm 0.2$ | $104.9 \pm 2.1$ | $-380 \pm 160$ | |
| 28 534 | 143–144 | $0.3 \pm 0.2$ | $106.1 \pm 2.4$ | $-480 \pm 180$ | |
| 26 207 | 165–166 | $0.6 \pm 0.2$ | $109.0 \pm 2.5$ | $-690 \pm 180$ | |
| 26 699 | 266–267 | $0.6 \pm 0.2$ | $97.0 \pm 2.0$ | $250 \pm 170$ | 1420–1680 AD |
| | | | | | 1770–1800 AD |
| | | | | | 1940–.. AD |
| 26 212 | 366–367 | – | $83.7 \pm 2.2$ | $1430 \pm 210$ | 340–800 AD |
| 26 704 | 465–466 | $1.2 \pm 0.2$ | $78.7 \pm 1.6$ | $1920 \pm 170$ | 160 BC–250 AD |
| 26 217 | 562–563 | $0.3 \pm 0.2$ | $70.6 \pm 2.2$ | $2800 \pm 250$ | 1390–790 BC |
| 26 710 | 665–666 | $0.5 \pm 0.2$ | $55.6 \pm 1.4$ | $4720 \pm 180$ | 3710–3330 BC |
| | | | | | 3220–3130 BC |
| 26 221 | 766–767 | $0.3 \pm 0.2$ | $49.0 \pm 1.9$ | $5740 \pm 310$ | 5000–4270 BC |
| 28 539 | 782–783 | – | – | | |
| 28 869 | 841–842 | $0.3 \pm 0.2$ | $27.2 \pm 1.3$ | $10\,450 \pm 380$ | 10 890–9820 BC |
| 26 722 | 866–867 | – | $26.6 \pm 1.4$ | $10\,630 \pm 430$ | 11 030–9980 BC |
| 26 231 | 970–971 | $0.3 \pm 0.2$ | $18.5 \pm 2.0$ | $13\,540 \pm 880$ | 15 780–13060 BC |
| 27 393 | 1066–1067 | $0.2 \pm 0.2$ | $13.7 \pm 1.4$ | $15\,960 \pm 840$ | 18 490–16330 BC |
| 26 236 | 1165–1166 | $0.6 \pm 0.2$ | $8.6 \pm 1.6$ | $19\,800 \pm 1500$ | 22 300–25800 cal BP |
| 27 386 | 1266–1267 | $-0.1 \pm 0.2$ | $5.6 \pm 1.5$ | $23\,200 \pm 2500/1900$ | |
| 27 387 | 1365–1366 | $0.0 \pm 0.2$ | $2.2 \pm 1.8$ | $30\,800 \pm 14\,000/4900$ | |
| 27 376 | 1469–1470 | $-0.1 \pm 0.2$ | $0.5 \pm 1.4$ | $42\,900 \pm xx/11\,000$ | |
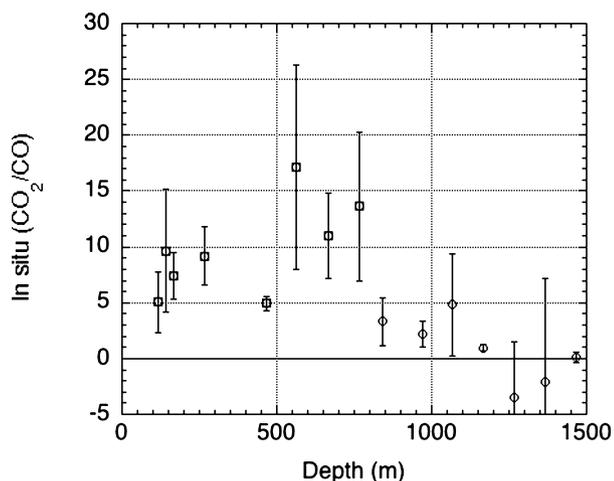


*Fig. 3.* The ratio of in situ produced $^{14}CO_2$ and $^{14}CO$ as a function of depth, indicating a variable ratio with depth.



*Fig. 4.* Comparison of measured and predicted activities, indicating a clear, though not one-to-one relationship.

and

$$I_a(t) = I_{m,0} e^{-\lambda t} (1 - e^{-\gamma t}). \qquad (5)$$

The air in the bubbles contains a natural $^{14}CO_2$ component with activity $A_0$ at $t = 0$, and an in situ component $I_a(t)$ with $I_a(0) = 0$. As the natural component also decays the total activity
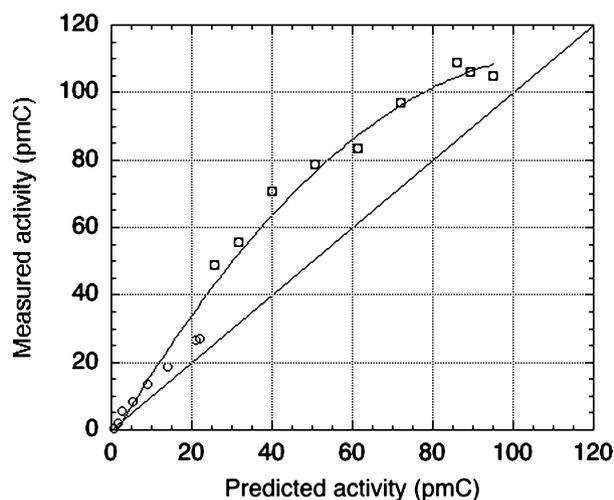
of $^{14}CO_2$, which is the measured quantity, can be described by:

$$A(t) = \left[ A_0 + I_{m,0} (1 - e^{-\gamma t}) \right] e^{-\lambda t} \qquad (6)$$

The constant $I_{m,0}$, which is called the 'saturation level' from now on, can be estimated in case of a constant accumulation rate
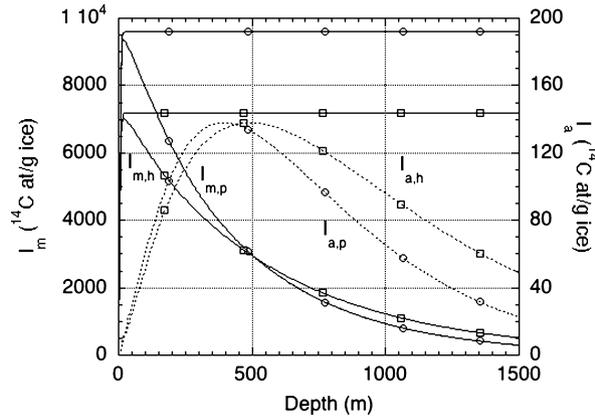
*Fig. 5.* Model performance in terms of the in situ component in the matrix ($I_m$) and in the air ($I_a$) for EDML ($P_0 = 285$ at $g^{-1}$, $\gamma = 6 \times 10^{-6}$ 1/yr) for Pleistocene conditions (indices $p$) and Holocene conditions (indices $h$). For reference we plotted the amount of $^{14}$C in the matrix without taking decay into account (horizontal lines). Note that the depth scale translates into different timescales for Pleistocene and Holocene, respectively, due to the different accumulation rates.

by the equation presented by Lal et al. (1987):

$$I_{m,0} = \frac{P_0}{\rho_i s / \Lambda - \lambda} (e^{-x\lambda/s} - e^{-x\rho_i/\Lambda}) \qquad (7)$$

in which $P_0$ denotes the $^{14}$C primary production rate (atoms $g^{-1}$ $yr^{-1}$) at the surface, $\Lambda$ the absorption mean free path of fast neutrons in ice (150 g cm$^{-2}$), $\rho_i$ the density of ice (0.9 g cm$^{-3}$), s the accumulation rate and $x$ the depth below the ice surface. The value of $I_{m,0}$ depends on the depth below the surface ($x$), but approaches a more or less constant level if $x$ is a few times $\Lambda$. This saturation level decreases with time due to decay (the first term between brackets in eq. 7). It depends on two variables, which are site specific, the primary production rate at the surface and the accumulation rate. The primary production rate is mainly a function of altitude (and latitude). Figure 5 shows typical Pleistocene and Holocene conditions for the EDML drill site. Elevation is assumed to be constant, but the Holocene accumulation rate of 6.6 cm we yr$^{-1}$ is reduced with a rather conservative reduction of 25% for Pleistocene conditions. The Figure clearly shows that decreased accumulation rates lead to higher saturation levels. In order to place these numbers in perspective one has to realize that modern air enclosed in ice contains between 800 and 1000 $^{14}$C at g$^{-1}$ ice depending on air volume and $CO_2$ concentration. This means that the saturation level is nearly an order of magnitude larger than the $^{14}CO_2$ level in the air bubbles.

What matters, however, is which fraction reaches the air bubbles used for the analyses and in which form ($^{14}$CO or $^{14}CO_2$) since the calculated saturation level refers only to the total $^{14}$C concentration in the matrix. Therefore, Fig. 5 also shows the amount $I_a$ of the in situ produced $^{14}$C, which has reached the air bubbles as $^{14}CO_2$, it is this quantity, which directly influences the $^{14}$C dating. The fraction $I_a$ is calculated for a value of $\gamma =$

$6 \times 10^{-6}$ (1 yr$^{-1}$) for the two cases in the figure. The figure shows that $I_a$ increases with depth to a maximum of about 140 at g$^{-1}$ ice due to the degassing and then reduces deeper down due to the $^{14}$C decay. The difference for Pleistocene and Holocene seem to be not very sensitive for the saturation level if the results are shown as a function of depth below the surface. However, a more realistic comparison is to show the model results as a function of time instead of depth, including the natural decay.

Figure 6 shows the sensitivity of the model for different values of the saturation level (which follow from the comparison with the data to be discussed below) and for different values of the degassing rate, $\gamma$, but now as a function of time. Clearly, the two parameters (saturation level and degassing rate) influence the results in a similar way (mainly because $\gamma$ is small), which means that fitting these free parameters to the observations will not provide unambiguous results for one of the parameters separately, but rather a line of optimal solutions. An increase in the saturation level can be compensated by a lower degassing rate and vice versa.
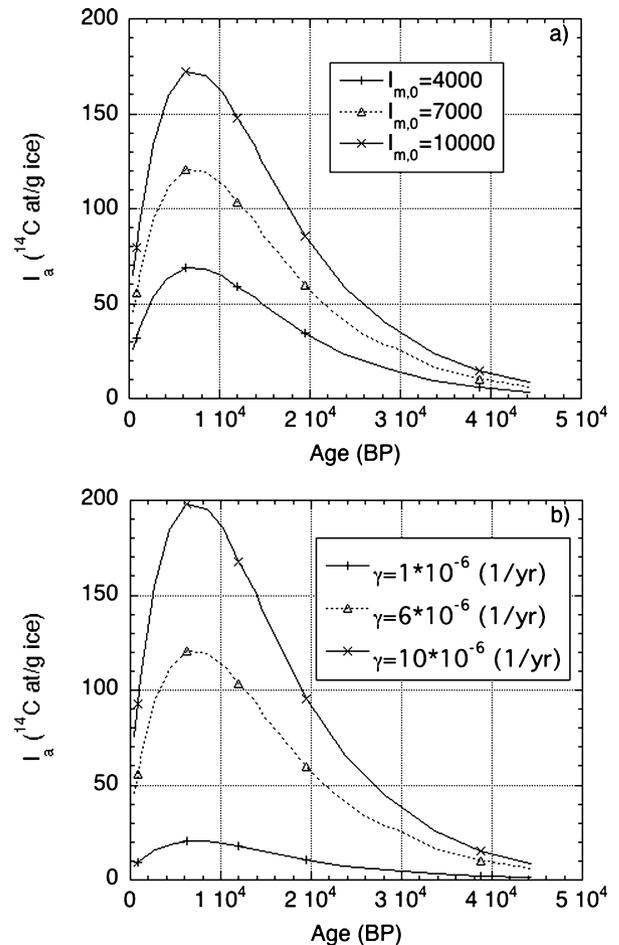


*Fig. 6.* Sensitivity of the in situ component in the air for different values of the saturation level for a fixed degassing rate $\gamma = 6 \times 10^{-6}$ 1 yr$^{-1}$ (a), as (a) but for different values of the degassing rate and fixed saturation level of 7000 at g$^{-1}$ ice (b).
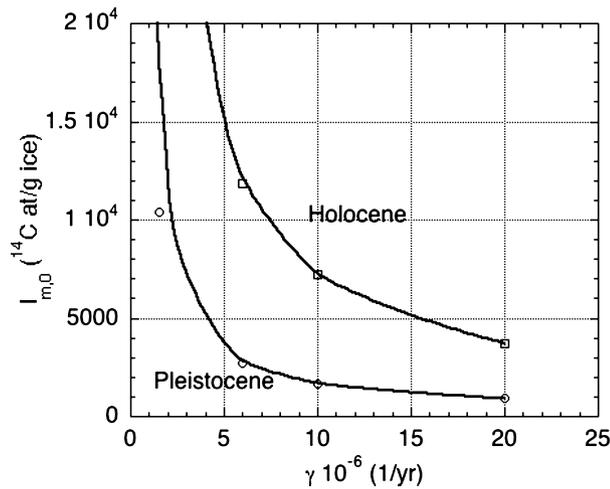
*Fig. 7.* Solution lines for the saturation level and degassing rate by tuning the model to the EDML data set. Each line contains the points, which yield the best solution for one of the two periods.

Finally, we fitted the model to the observations with the degassing rate and the saturation level as free parameters. Many scenarios have been tested but they all showed a clear improvement when different values for the saturation level were used for the Pleistocene and Holocene samples. Similar values for the degassing rate and saturation level over both Holocene and Pleistocene performs statistically significantly worse than separating the data set in a Pleistocene and a Holocene part. The division into two periods is justified by the large difference in temperature and accumulation, causing different saturation levels as well as presumably different degassing rates. Figure 7 shows the optimal solution lines for the Pleistocene and for the Holocene period. Pleistocene samples are less affected by in situ production (see Fig. 2) and the solution line is therefore below that of the Holocene. Points on these lines are statistically of identical quality in terms of the root mean squared error (RMSE). For the Holocene period we find a RMSE of 20 at $g^{-1}$ ice and for the Pleistocene period of 5 at $g^{-1}$ ice, which corresponds roughly to 1.5 and 0.33 pmC, respectively. The $1\sigma$ ranges pinpointing single values as optimal values for the constants can be achieved by realizing that the saturation level follows from different climate conditions imposed in eq. (7). If one adopts an accumulation rate of 6.6 cm we $yr^{-1}$ for the Holocene and 4.6 cm we $yr^{-1}$ for the Pleistocene the saturation levels can be calculated as 7200 and 10400 at $g^{-1}$, respectively. This then implies, the value for the remaining free parameter, the degassing rate. We found $= 1 \times 10^{-5}$ $(1\ yr^{-1})$ for the Holocene and $\gamma = 1.8 \times 10^{-6}$ $(1\ yr^{-1})$ for the Pleistocene both points on the lines in Fig. 7. So, the degassing rate during the Pleistocene is lower than during the Holocene, which might intuitively be explained by the lower temperatures.

The $^{14}$CO measurements (Fig. 1) seem to indicate a decrease of activity over time, which cannot be explained by decay only. One might speculate that this is due to the fact that part of the

in situ produced $^{14}$C reacts to $^{14}$CO and a part to $^{14}$CO$_2$. Little is known about the mechanism of formation of $^{14}$CO and $^{14}$CO$_2$, maybe it is temperature dependent and such a dependency could affect the $^{14}$CO$_2$ in the air bubbles. So as a thought experiment we calculated the consequences of varying the ratio between the two components over time. Incorporating the simplest form of this effect into our model leads to a change of eq. (5) to:

$$I_a = I_{e,CO_2} + I_{a,CO} \tag{8a}$$

$$I_{a,CO_2} = (1 - r)I_a \tag{8b}$$

$$I_{a,CO} = r I_a \tag{8c}$$

in which the subscript CO$_2$ indicates the $^{14}$C production, which leads to $^{14}$CO$_2$ and the subscript CO indicates the part ending in $^{14}$CO. The separation between the two fractions is given by the ratio $r$, a scaling parameter between zero and one, variations in degassing rate of $^{14}$CO and $^{14}$CO$_2$ are neglected. This implies a constant ratio for the in situ component in the fractions, which follows from the ratio $(r)$. Fitting the data with this extended model yields a value of approximately 0.12 for $r$ in the Holocene and 0.45 in the Pleistocene. This extended model has five parameters instead of four ($I_{m,p}$, $I_{m,h}$, $\gamma_p$, $\gamma_h$, $r$), but uses also the $^{14}$CO data, which increases the number of data points used from 17 to 32. However, the fitting results for the primary four parameters ($I_{m,p}, I_{m,h}, \gamma_p, \gamma_h$) are hardly affected. Given the fact that the $^{14}$CO concentrations are barely above background values, we consider this further specification of the model too speculative at this stage.

Figure 8 shows a comparison of the modelled activity including the natural decay and the in situ production as a function of the measured $^{14}$CO$_2$ activity (Fig. 8a). The modelled activity is obtained by applying eq. (6) as explained above. The bias between measured activity and expected activity, as shown in Fig. 4 clearly disappears. The proposed model removes the bias by producing the right amount of in situ molecules in the air bubbles. As a consequence the $^{14}$C age based on the model and the expected values are also in mutual agreement, as shown in Fig. 8b.

Of course we cannot claim that the degassing rate is a universal constant but by assigning an arbitrary error of 25% to the calculated in situ fraction of CO$_2$ in the air bubbles we can estimate the error in the age of the air. So this experiment only serves the purpose to show what one might expect in terms of age estimates if we are able to estimate the in situ fraction within this 25% range. Results in terms of calendar years are shown in Figure 8c. The error in the modelled age increases over time due to the decay process, but the effect of the errors in the in situ calculation are highest in the Holocene (see Figs. 6 and 7). As a result the combined error has around 13 kyr a local maximum of 3 kyr and decreases then back to 1.2 kyr. Beyond 20 kyr the error increases again as a result of the decay process.
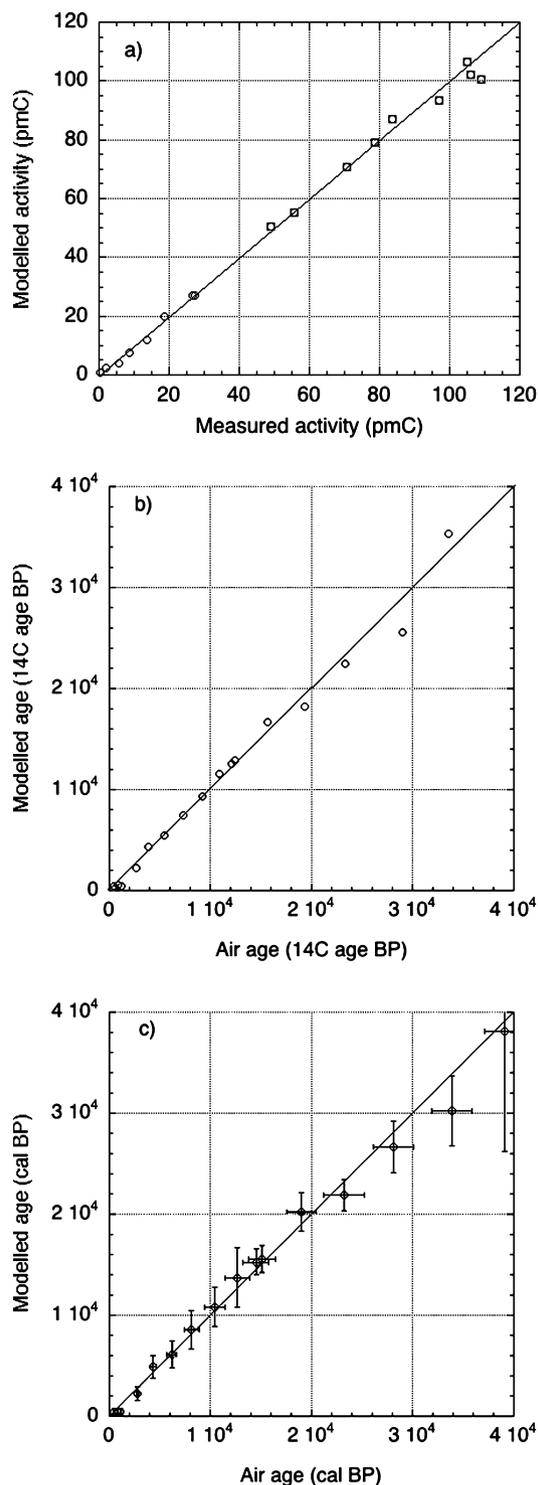
*Fig. 8.* Results of the modelled activity as a function of the measured activity (a). Model parameters are $\gamma = 6 \times 10^{-6}$ (1 yr$^{-1}$) and $I_{m,0} = 7200$ (at g$^{-1}$ ice) for the Holocene and $\gamma = 1.8 \times 10^{-6}$ 1 yr$^{-1}$ and $I_{m,0} = 10\,400$ (at g$^{-1}$ ice) for the Pleistocene. The resulting comparison of air ages in $^{14}$C years is shown in b. Assigning an error of 25% in the calculation of the in situ production yields the corrected calendar ages and errors shown (c).

The result of the model is satisfactory. Observations and expected values are within the uncertainties one might expect, but there is not yet an independent data set to validate the model. The model parameters (degassing rate and saturation level) are tuned to the EDML data set and in order to date independently of any expected values these parameters need to be universal, but no other data are yet available. Variations might arise from quantities like the impurity content and ice structure which are hard to quantify, on the other hand it might well be possible that elevation, temperature and accumulation rate are controlling the degassing rate as well as the saturation level. As long as there are no other data available the 25% error estimate is clearly arbitrary.

Although independent verification of the model is not yet possible one can at least argue that the low $^{14}$CO values presented by Van der Kemp et al. (2000) are not in contradiction with the proposed model. However, they only analysed nearly modern samples, which are not very conclusive in view of the timescale of the degassing from the matrix. The interpretation of the result by Van der Kemp et al. (2000) was that there was no appreciable in situ production just below pore close off in the air bubbles, and hence radiocarbon dating of ice is possible. Here, we have shown that this argument does not hold. EDML samples also show nearly no in situ production just below pore close off, but consequences of in situ do nevertheless show up at larger depths. It was this observation, which has led to the degassing theory formulated in this paper.

Finally we like to indicate regions in Antarctica where in situ production can be ignored. In situ levels depend on accumulation rate, the higher the accumulation the lower the in situ production, and on the in situ saturation level, which depends on the primary production rate, which is elevation dependent, the higher the elevation the more in situ production. Taking these effects into account leads to Fig. 9, which indicate the areas in Antarctica where in situ production is low. The figure shows the error due to measurement precision as a reference benchmark as a function of the age of the ice. As long as the error due to the in situ production remains under the line of the measuring error, the effect of the in situ production is negligible, which is the case in the low-lying areas ($P_0$ low) with reasonable accumulation rate, both features leading to low values for $I_{m,0}$. The figure shows that $^{14}$C dating of ice from the high and dry Antarctic plateau will always suffer from in situ production and its degassing of its products from the matrix.

## 5. Conclusions

Results for this core show that background levels are not the main concern for dating, which is the primary goal, but rather the in situ production leading to enhanced levels of $^{14}$CO$_2$ in air bubbles enclosed in ice. Accurate dating of ice from an accumulation zone is therefore only possible if the contribution from in situ production is negligible. This might be the case for some particular areas. It is shown here that on the Antarctic plateau,
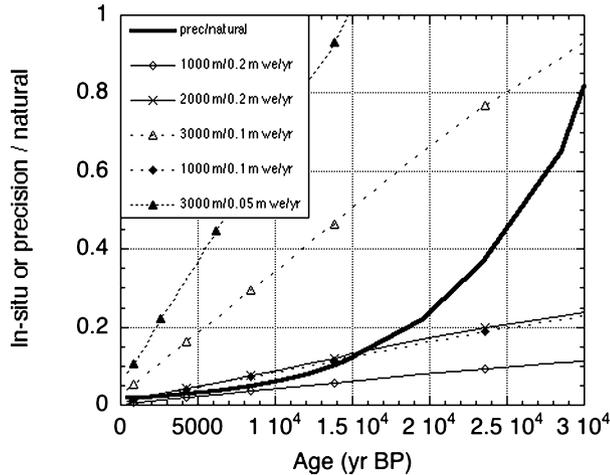
*Fig. 9.* The activity of in situ produced $^{14}$C, for different accumulation rates and elevations, is shown as a fraction of the naturally enclosed $^{14}$C in the air bubbles. For reference (bold line) we also show the measuring error as a fraction of that of the naturally enclosed $^{14}$C in the air bubbles. In situ production can be neglected if its effect is smaller than the measuring error (bold line). One can observe that on the high and dry interior parts of Antarctica in situ production in combination with degassing from the matrix is an important process. Only for low elevation and large accumulation rate in situ production is of minor importance.

with its high intensity of cosmogenic radiation and its low accumulation rates, in situ production cannot be neglected. In this paper we propose a model to correct for the in situ production. Application of the model allows for dating if the error in the in situ correction are smaller than 25%, because then measured $^{14}$CO$_2$ activities can be reliably be corrected for in situ produced and released $^{14}$CO$_2$. The validity of our model remains to be tested by measurements on other ice cores.

# 6. Acknowledgments

# 7. Appendix

To improve the processing and measuring reliability of CO$_2$ samples, the amount of CO$_2$ extracted from the ice sample is increased to 200 $\mu$gC by adding a $^{14}$C-free, diluent CO$_2$ gas with a known $\delta^{13}$C. A fair approximation of the original CO$_2$ sample activity is deduced from the diluted CO$_2$ sample measurement, via a calculation using mass conservation. The complete calculation of the normalized activity of the original CO$_2$ sample, however, is not straightforward due to the isotope fractionation in AMS.

The AMS simultaneously measures the $^{14}$C/$^{12}$C and $^{13}$C/$^{12}$C ratio of the diluted CO$_2$ sample (Van der Plicht et al., 2000). During the measurement on these somewhat smaller samples, the temperature of the cesium reservoir of the ion source is raised by 2–3 °C compared to its value for measurements on normal sized samples, to optimize the yield. The $^{14}$C/$^{12}$C ratios of the diluted CO$_2$ sample and line blanks are reported relative to the HOxII standard and normalized to $\delta^{13}$C $= -25‰$ (Mook and Van der Plicht, 1999). Then the activity of the diluted CO$_2$ sample is corrected for the mean line blank activity and transformed into a non-$\delta^{13}$C corrected activity ($a_{\text{tot}}$).

If the sample had not been diluted, the AMS would have measured the original CO$_2$ sample activity. This activity is represented by $a_{\text{org}}$, which is found from mass conservation:

$$a_{\text{org}} = \frac{a_{\text{tot}} - x \cdot a_{\text{dil}}}{1 - x}, \tag{A1}$$

where $x = m_{\text{dil}}/m_{\text{tot}}$, is the mass ratio of the diluent gas and the diluted CO$_2$ sample, $a_{\text{dil}}$ would be the activity of the diluent gas, had it been measured by the AMS. In this case $a_{\text{dil}} = 0$. The $\delta^{13}$C value of the original CO$_2$ sample as measured by the AMS (represented by $\delta^{13}$C$_{\text{org}}$) is found from the AMS measured $\delta^{13}$C for the diluted CO$_2$ sample ($\delta^{13}$C$_{\text{tot}}$):

$$\delta^{13}\text{C}_{\text{org}} = \alpha_{\text{AMS}} \left[ 1 + \frac{\left( \frac{1+\delta^{13}\text{C}_{\text{tot}}}{\alpha_{\text{AMS}}} - 1 \right) - x\delta^{13}\text{C}_{\text{dil,IRMS}}}{1 - x} \right] - 1 \tag{A2}$$

where $\delta^{13}$C$_{\text{dil,IRMS}}$ is the actual $\delta^{13}$C of the diluent gas, which is measured with a stable Isotope Ratio Mass Spectrometer (IRMS). Here, the mean AMS fractionation factor for the standards ($\alpha_{\text{AMS}}$) is assumed to be valid for the other samples as well.

Alternatively, $\alpha_{\text{AMS}}$ can be deduced on a sample-to-sample basis if the $\delta^{13}$C of the diluted CO$_2$ sample is also measured with a stable IRMS. This $\delta^{13}$C-value is more precise and results in a smaller error in the activity. Hence, it is used at the CIO if it is available.

The activity of the original CO$_2$ sample is normalized to $\delta^{13}$C $= -25‰$:

$$a_{\text{org,N}} = a_{org} \left[ \frac{0.975}{1 + \delta^{13}C_{\text{org}}} \right]^2 \tag{A3}$$
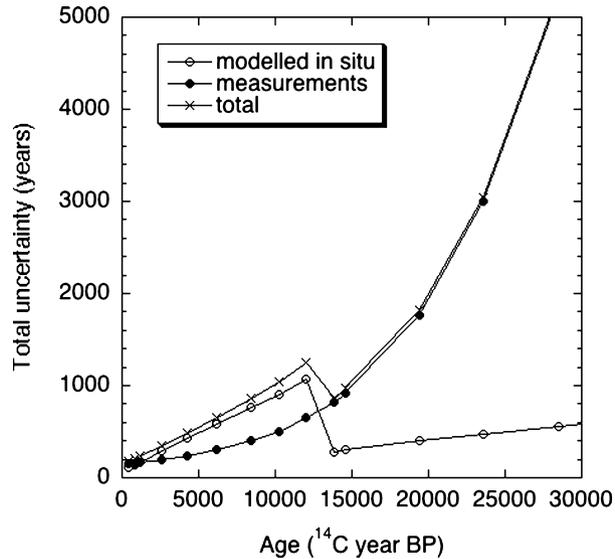
*Fig. 10.* The uncertainty of the dating as a function of the age of the samples given the measurement error and an arbitrary error of 25% in the calculation of the in situ production. Before 12 000 years the uncertainty is dominated by the in situ production. After 15 000 years the uncertainty is dominated by the measurement error.

with $a_{org,N}$ representing the $\delta^{13}C$-corrected activity of the $CO_2$ extracted from the ice sample, had it been analysed in its pure form. The age of the ice sample is found from this normalized activity:

$$age = -8033 \ln(a_{org,N}) \tag{A4}$$

Due to the dilution with a $^{14}C$-free $CO_2$ gas, all samples appear to be relatively old. Therefore, the uncertainty in the line blanks ($= \sim 0.17$ pmC) is the dominant contribution to the error for most of the $CO_2$ samples. The activity of the original $CO_2$ sample is approximately equal to the measured activity of the diluted sample divided by $1 - x$. See eq. (A.1), with $a_{dil} = 0$. This implies that the error scales with the same factor.

In the present experimental set-up with $x = 0.85$, the age limit is therefore about 36 000 $^{14}C$ years:

$$\sigma_{a_{org,N}} = \frac{0.17\,pMC}{1-x} = 1.1\,pMC \tag{A5}$$

The standard deviation in the $^{14}C$ ages of EDML sample 165–166 to 1165–1166 is approximated by:

$$\sigma_{age} = -8033 \frac{\sigma_{a_{org,N}}}{a_{org,N}}. \tag{A6}$$

For the older samples the standard deviation in the $^{14}C$ age is calculated from the activities $a_{org,N} + \sigma(a_{org,N})$ and $a_{org,N} - \sigma(a_{org,N})$.

The uncertainties in the $^{14}C$ ages of the ice samples depend on the accuracy of the in situ calculation and on the measurement

precision. This is shown in Fig. 10. In the Holocene part the uncertainty is mainly caused by the correction for in situ production. In the Pleistocene part this is far less important and the uncertainty is determined by those in the measurements. If the $CO_2$ samples would have been twice as large, the uncertainties in the Pleistocene would be nearly twice as low and competitive with those of other dating techniques.

## References

De Jong, A. F. M., Alderliesten, C., van der Borg, K., van der Veen, C. and van de Wal, R. S. W. 2004. Radiocarbon analysis of the EPICA Dome C ice core: no in-situ $^{14}C$ from the firn observed. *NIMB* **223-224**, 516–520.

Jull, A. J. T., Lal, D., Donahue, D. J., Mayewski, P., Lorius, C. and co-authors. 1994. Measurements of cosmic-ray-produced $^{14}C$ in firn and ice from Antarctica. *NIMB* **92**, 326–330.

Lal, D. and Jull, A. J. T. 1990. On determining ice accumulation rates in the past 40000 years using in-situ cosmogenic $^{14}C$. *GRL* **17**(9), 1303–1306.

Lal, D., Nishiizumi, K. and Arnold, J. R. 1987. In-situ cosmogenic $^3H$, $^{14}C$ and $^{10}Be$ for determining the net accumulation and ablation rates of ice sheets. *JGR* **92**(B6), 4947–4952.

Mook, W. and Van der Plicht, J. 1999. Reporting $^{14}C$ activities and concentrations. *Radiocarbon* **41**, 227–239.

Roessler, K. 1988. Hot atom chemistry in space-simulation with nuclear methods. *Radiochim. Acta* **43**, 123–125.

Reimer, P. J. M., Baille, M. G. L., Bard, E., Bayliss, A., Beck, J. W. and co-authors. 2004. INTCAL04 terrestrial radiocarbon age calibration, 0-26 cal kyr BP. *Radiocarbon* **46**(3), 1029–1058.

Smith, A. M., Levchenko, V. A., Etheridge, D. M., Lowe, D. C., Hua, Q. and co-authors. 2000. In search of in-situ radiocarbon in Law Dome ice and firn. *NIMB* **172**(1), 610–622.

Van de Wal, R. S. W., van Roijen, J. J., Raynaud, D., van der Borg, K., de Jong, A. F. M. and co-authors. 1994. From $^{14}C/^{12}C$ measurements towards radiocarbon dating of ice. *Tellus* **46B**, 94–102.

Van der Kemp, W. J. M., Alderliesten, C., Van der Borg, K., Holmlund, P., De Jong, A. F. M. and co-authors. 2000. Very little *in-situ* produced radiocarbon retained in accumulating Antarctic ice. *NIMB* **172**, 632–636.

Van der Kemp, W. J. M., Alderliesten, C., van der Borg, K., de Jong, A. F. M., Lamers, R. A. N. and co-authors. 2002. In-situ produced $^{14}C$ by cosmic ray muons in ablating Antarctic ice. *Tellus* **54B**, 186–192.

Van der Plicht, J. 1993. The Groningen radiocarbon calibration program. *Radiocarbon* **35**(1), 231–237.

Van der Plicht, J., Wijma, S., Aerts, A. T., Pertuisot, M. H. and Meijer, H. A. J. 2000. The Groningen AMS facility : status report. *NIMB* **172**, 58–65.

Van Roijen, J. J. 1996. *Determination of ages and specific mass balances from $^{14}C$ measurements on Antarctic surface ice*. PhD thesis, Utrecht University, The Netherlands, 119 pp.

Van Roijen, J. J., Bintanja, R., Van der Borg, K., Van den Broeke, M. R., De Jong, A. F. M. and co-authors. 1994. Dry extraction of $^{14}CO_2$ and $^{14}CO$ from Antarctic ice. *NIMB* **92**, 331–334.